INCORPORATION OF STIMULI-RESPONSIVE BACTERIA IN MICROFLUIDIC DROPLETS

by

KENGELLE Q. CHUKWURAH

(Under the Direction of Eric Freeman)

ABSTRACT

Cellular membrane mimics offer an exchange between two neighboring aqueous droplets. This regulated exchange may prove useful for controlling the various agents in aqueous micro-environments. The following works focuses on characterizing the bacterial response within a synthetic cellular environment. In the droplet interface bilayer (DIB) approach, aqueous micro-droplets deposited in an oil reservoir with dissolved lipids are coated with lipid monolayers and arranged into artificial cellular networks. In this study, the response of bacteria within asymmetric droplet networks separating the bacteria and a chemoattractant highlighted the efficacy of the DIB approach.

INDEX WORDS: Cellular Membranes; Droplet Interface Bilayer; Escherichia Coli

INCORPORATION OF STIMULI-RESPONSIVE BACTERIA IN MICROFLUIDIC DROPLETS

by

KENGELLE Q. CHUKWURAH

B.S., The University of Georgia, 2013

A Thesis Submitted to the Graduate Faculty of The University of Georgia in Partial Fulfillment of the Requirements for the Degree

MASTER OF SCIENCE

ATHENS, GEORGIA

2016

INCORPORATION OF STIMULI-RESPONSIVE BACTERIA IN MICROFLUIDIC DROPLETS

by

KENGELLE Q. CHUKWURAH

Major Professor: Eric Freeman
Committee: Yajun Yan
Andrew Sarles

Electronic Version Approved:

Suzanne Barbour
Dean of the Graduate School
The University of Georgia
May 2016

DEDICATION

I would like to dedicate this documentation to my colleagues, friends, and family:

My colleagues in the Biomembrane Engineering were relentlessly supportive. Alongside them, all things were possible, no matter the depth of knowledge required, the skill set demanded, or the difficulty of the task. With dedication and confidence, there was hardly a matter we could not face. Memories of my colleagues will remind me to persevere through everything and always leave time to play a little soccer.

My friends always filled me with joy each day of the week. I have realized that throughout any professional pursuit in life, friends have the most lasting impact. My friends helped me realize that there is life worth living outside of the laboratory. These friendships also challenged me to find meaning in the small things, like coffee breaks and spontaneous conversations.

The Chukwurah family was the fuel of my work throughout the MS program. Their unprompted words of wisdom and undeserved lyrics of praise propelled my determination for success. My sister always reminded me, “Even when it can’t be done, do it anyways.” She, along with my father, mother, and brother, believed I was capable of solving any problem that had come my way. Many of my accomplishments presented in this thesis found root in this notion. From them, I learned there is no one or thing that can stand in the way of a person whom is unafraid to undoubtedly attempt, fail, learn and attempt again.

ACKNOWLEDGEMENTS

Many people have contributed to the following works. I would like to acknowledge a few that were highly influential towards the completion of the MS program at UGA. First, I would like to give regards to my advisor Dr. Eric Freeman, who was a continual source of advice and encouragement. My committee members, Dr. Yajun Yan and Dr. Andrew Sarles, provided great advice for my research and career endeavors. I greatly appreciated my professor, Dr. Kisaalita, whom was a reliable friend, mentor, and profound lecturer. Then, I must remark the ideas and helpfulness of my colleagues and friends in the Biomembrane Engineering Lab. Last, I would like to acknowledge my family members, Charlene, Kenneth, Kenneth Jr., and Crystal Chukwurah, for their much needed love and support throughout my graduate studies.

TABLE OF CONTENTS

Page

LIST OF TABLES

Page

LIST OF FIGURES

Page

CHAPTER 1

INTRODUCTION

1.1 Purpose of the Study

The thesis presents a study of interactions between a model cellular membrane and bacteria. Here is an exploration of host-pathogen interactions, the host being a model cellular membrane and the pathogen being a bacterial strain of *Escherichia coli* (*E. coli*). An analysis of the interaction of bacteria with a model cellular membrane broadens comprehension of the model's physiological relevance as well as the bio-molecular mechanisms that occur at the cell level.

1.2 Expected Results

The bacteria may effect the cellular membrane formation and stability. In the microfluidic droplets, *E. coli* may retain their motility and potentially induce the interfacial membrane's collapse upon interaction. Expectedly, the *E. coli* may move faster in the presence of an attractive chemical or move towards a chemoattactant in a given area. Therefore, the resulting bacterial motion will demonstrate whether bacteria are capable of sensing transmembane chemical gradients.

CHAPTER 2

LITERATURE REVIEW: LIPID BILAYER AND *ESCHERICHIA COLI*

2.1 Lipid Bilayer

Fundamentals of the Cellular Membrane. The cellular membrane acts as a barrier for all cells and the organelles within cells. The membrane typically protects the cell from invaders, facilitates cell communication with neighboring cells, and allows molecule transportation in and out of the cell. The cellular membrane is selectively permeable to ions and organic molecules. Glucose and polar molecules, like potassium and sodium ions, do not cross the membrane easily, whereas, water and non-polar molecules, like oxygen can freely pass through the membrane. Such molecules are quite essential for the cell, so the glucose and polar molecules cross the cellular membrane through embedded protein channels [8].

Phospholipid molecules and lipids are the primary composite of cellular membranes. The composites arrange as follows: the phospholipid molecules as head groups and the lipids as tails (Figure 1). Strong hydrophobic interactions induce an attraction among the tail groups. In addition, the tails naturally refrain from aqueous environments, while the hydrophilic head groups have the opposite response. The combination of these composites into one structure is called a lipid bilayer. The lipid bilayer persuades molecules to attach atop or insert inside the bilayer. Alec Bangham and Robert Horne observed these active concepts of the bilayer under electron microscopy in 1962 [9]. Today, lipid bilayer vesicles are engineered to function as

devices for carrying essential therapeutic agents, such as drugs and genetic material, throughout the body [10]. The lipid bilayer offers a stable material for various applications in regenerative medicine and material science.

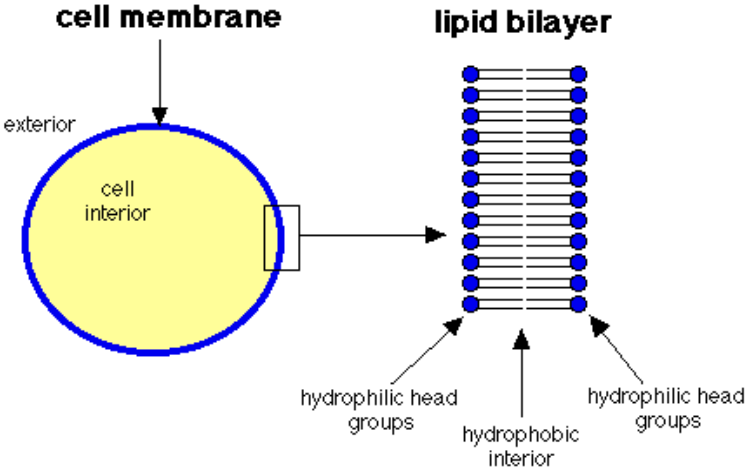

Figure 1 - Cell Membrane and Lipid Bilayer. Phospholipids are the primary composite of cell membranes. They consist of a hydrophilic head group and hydrophobic tail (interior) [1].

The Mosaic of the Lipid Bilayer. Each side of the bilayer is called a leaflet [11]. The outer leaflet faces the extracellular fluid while the inner leaflet faces the cell cytoplasm. Researchers have found that these leaflets of a cell membrane vary in composition for all cell types. For instance, a red blood cell membrane contains 53% phospholipids, whereas the myelin of neural cells has 62% of the same lipid type [12, 13]. The lipid composition also varies within leaflets of the same membrane. Red blood cell membranes are composed of 4 different phospholipids (Figure 2) [2].

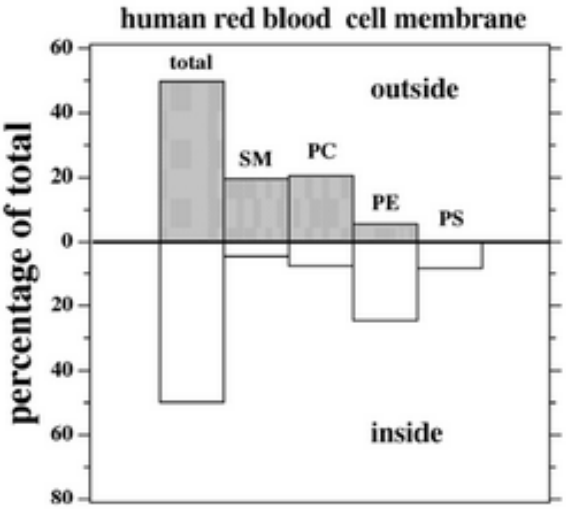

Figure 2 - Lipid Composition. The cell membrane of red blood cells is composed of varying concentrations of phospholipids on its inner and outer leaflet. [2]

Alongside the variances in lipid composition, the proteins in the membrane also characterize the lipid bilayer of the cells. The proteins may embed either on the surface or inside the cell membrane. The molecules and ions that cannot pass through the membrane with ease, typically utilize the proteins as a channel to get into or out of the cell. The channels can either open and close freely or be activated with protein receptors and energizer molecules, like adenosine tri-phosphate (ATP).

2.2 Artificial Membrane Formation Techniques

Model cellular membrane systems allow for the study of cellular interactions in a controlled environment. The models also broaden studies of the lipid bilayer structure and function.

Montal-Mueller or Lipid Folding Technique. A lipid dissolved in an organic solvent is spread across a hydrophobic material (Figure 3). A septum splits the lipid layer into two chambers filled with an electrolyte solution. When the ionic strength of the electrolyte solution is above 100mM, it produces an electrical conducting solution [14]. The electrolyte is shifted upwards to form a lipid bilayer across an aperture, which is a small gap of a septum. Once stabilized, the membrane lasts for several hours [14, 15]. The bilayer is typically very delicate but may be used to study a single pore for channel gating [16].

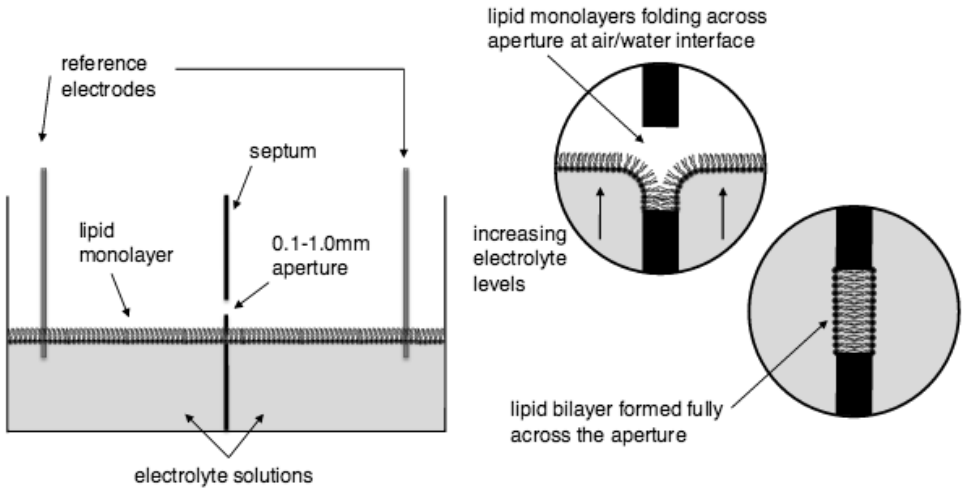

Figure 3 - Lipid Folding Technique. A layer of lipids is spread atop an electrolyte solution. A septum separates the lipids into two wells. The electrolyte solution is shifted upwards, triggering a bilayer formation at the aperture.[3]

Vesicle Fusion. The liposome is a lipid bilayer vesicle. This vesicle may be used to carry small material such as drugs, enzymes, or DNA. Strong interactions of the lipid

molecules make the vesicle hard to rupture. However, vesicle fusion opens up this vesicle and forms a planar lipid bilayer (Figure 4).

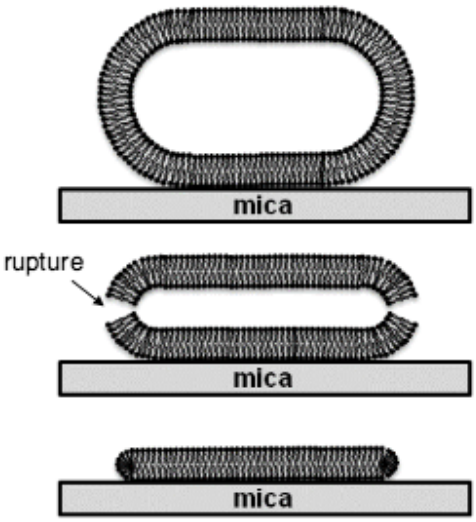

Figure 4 - Vesicle Fusion. A lipid bilayer vesicle, also called a liposome, can be ruptured on a hydrophilic substrate, like mica, to form a continuous bilayer. A portion of the bilayer that is adhered to the substrate is used for further studies, while the rest is rinsed away with a buffer. [3]

Placing a liposome vesicle on a clean, hydrophilic material, such as gold, glass, mica, or quartz, induces this rupture [17]. Vesicle fusion is a very common technique [18]; however, researchers struggle to study the activity of integral membrane proteins because the proteins would become immobile due to their adhesion to the substrate. However, a polymer cushion on the substrate has improved this method [19]. Vesicle fusion aided

studies of bilayer composition and orientation according to researchers, Visco, Chiantia, and Schwille [20].

2.3 Droplet Interface Bilayer Technique

The droplet-interface bilayer (DIB) technique designed by Hagan Bayley's laboratory in 2008, allows for the rapid construction of model biological and cellular membranes through self-assembly principles[15]. Lipids act as a natural surfactant when dissolved in an oil-water emulsion. They coat the aqueous emulsions with an ordered lipid monolayer. These lipid-coated emulsions form an interfacial lipid bilayer when brought into contact. DIBs are studied as potential biologically inspired materials, recognizing that the cellular membrane is capable of responding to a wide variety of stimuli. This approach to synthetic biology is often dubbed "bottom-up", wherein a synthetic biological system is carefully created from individual components. Previous works explored the DIB technique for sensing [21], actuation [22], and energy conversion[23].

2.4 The Advancement of the Model Lipid Bilayer

This study uses electrophysiology to replicate cellular transmembrane activity. The model membrane is engineered to respond in a particular manner by adjusting the membrane potential or the ions placed around the membrane. Proteins and channels may be inserted into the membrane, and their dependency on an applied voltage may be studied. As an example of this, Graham Taylor observed the influence of temperature on membrane peptides, alamethicin in particular [4]. Fluctuations in the membrane conductance confirmed the formation of a single channel in both a symmetric

and asymmetric bilayer (Figure 5). The open channel facilitated the exchange of fluid and charge across the membrane.

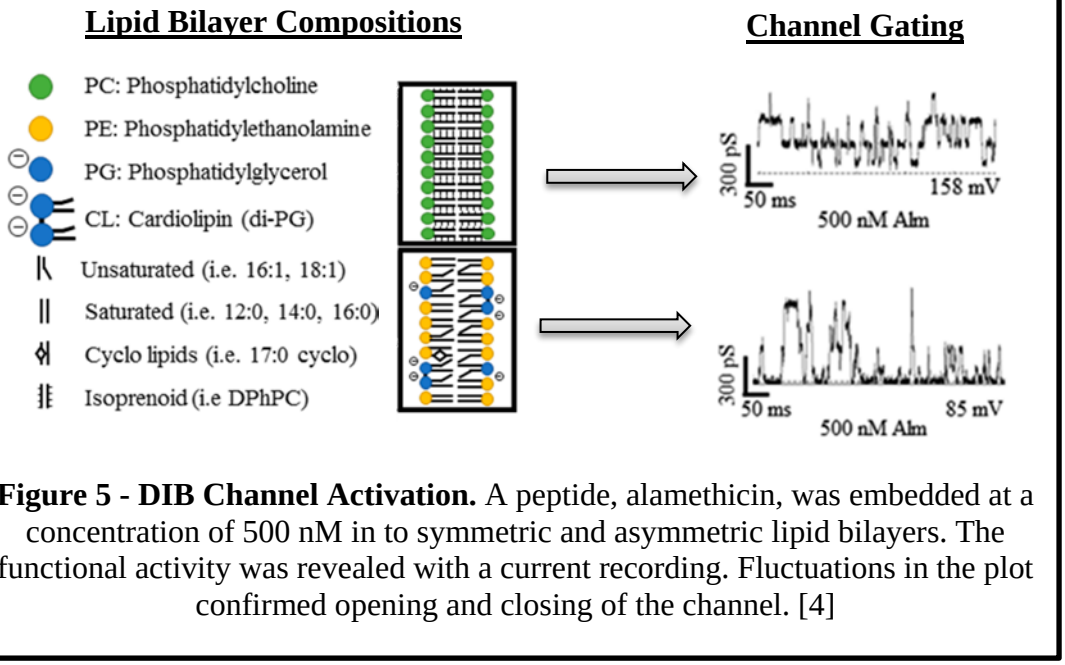

Figure 5 - DIB Channel Activation. A peptide, alamethicin, was embedded at a concentration of 500 nM in to symmetric and asymmetric lipid bilayers. The functional activity was revealed with a current recording. Fluctuations in the plot confirmed opening and closing of the channel. [4]

2.5 Bacteria Trigger Additional Responses in the DIB

Bacteria thrive almost anywhere, from the soil of the ground to the gut of a human body [24, 25]. They are ten-times more abundant in the human body than the total amount of human cells [26]. *E. coli* is a widely used gram-negative bacterium. It typically serves as a model organism in experiments that wish to validate a hypothesis before up-scaling to larger organisms. The *E. coli* genome can be engineered through transformations, mutations, and knockouts performed in a laboratory setting. For instance, Maximilian Weitz used green fluorescent protein (GFP) to transform *E. coli* cells so that he could observe when the cells received a particular molecule [6] (Figure 6).

The ability to observe the cells helped him analyze the induction patterns of *E. coli* encapsulated in water-in-oil droplets surrounding an activator-filled droplet. Moreover, he studied the interaction of an inducer molecule, Nacyl-L-homoserine lactones (AHL) in the network of droplets. AHL binding to a pLuxR promoter of the bacteria genome activated the expression of the GFP. In result, the AHL molecules, placed at the center of many bacteria-filled droplets, diffused across the interfaces of the droplets and activated the GFP of the bacteria. The ability of the molecules to diffuse between compartments confirmed chemical communication channels, and the expression of the GFP signified computational bacteria that process molecular input signals. These findings may be applied to the DIB.

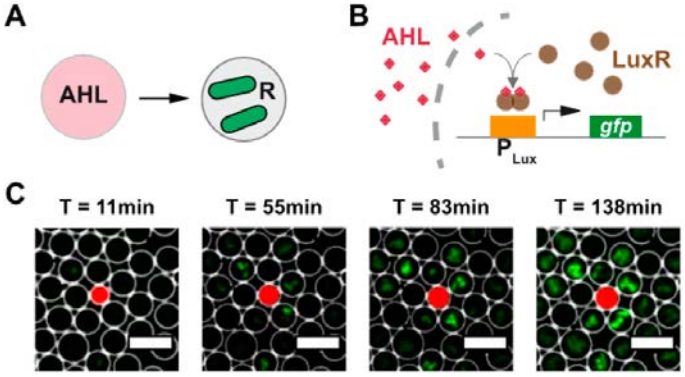

Figure 6 - Computational Bacteria. (A) Receiver bacteria in the presence of AHL reservoir droplets, which activate expression of GFP by attaching to LuxR promotors (B), is captured in a time series beginning at 11 minutes and ending after 138 minutes. (C). [6]

2.6 Motility and Chemotaxis

Flagellar Motors. In this study, the DIB shows off certain characteristics of the *E. coli*, such as their motility and attraction to chemicals. Biologists term their styles of motility as swimming, twitching, and gliding [27]. The flagellar tails of the *E. coli* cells determine this behavior. Moreover, the orientation, length, and quantity of the flagellar tails around the cell affect the style and direction the cell moves. For instance, a plethora of tails oriented all over the cell may cause the cell to spin uncontrollably in an attempt to swim in a desired direction. Whether the tails propel in the clockwise (CW) or counterclockwise (CCW) direction also influence the cell's style of motility. When the tails spin in the CW direction, they become unorganized which provokes an erratic, tumble motion, whereas, when the tails spin in the CCW direction, the cells bundle into a filament that pushes the cell in a forward run.

In 2013, Hugo Wioland studied the motility of B. subtilis, a gram-positive bacterium, in a two dimensional microenvironment. He adjusted the size of droplet emulsions from 10 micrometers (μm) to 1 millimeter (mm) after submerging them in mineral oil. He coated the droplets with a lipid, diphytanoyl phosphatidylcholine, to maintain stability. Wioland observed a collective motion of the cells. They appeared to circumnavigate the center of the droplet for as long as oxygen was present [7, 28]. Uniquely, the cells at the boundary moved in an opposite direction from the cells found near the center of the droplets (Figure 7). Presumably, the boundary curvature of the droplet and the cells' interaction with the droplet surface caused this motility pattern. The bulk motion of the cells induced a shear flow that twisted the cells at the boundary in a different direction [7]. Furthering this experiment in 2014, Enkeleida Lushi confirmed

the cells' swimming direction with studies of the flagellar orientation [29]. The position of the flagella was a key factor in determining how the bacteria swam.

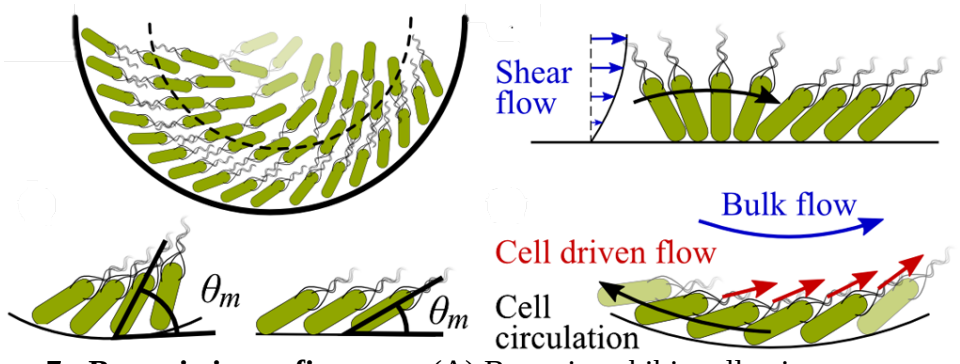

Figure 7 - Bacteria in confinement. (A) Bacteria exhibit collective movement in a direction that is dependent on the cell's placement in a two dimensional microenvironment. (B-C) A shear flow causes the bacterial cells at the boundary to bend at an angle and circulate the environment at that angle. (D) Cells at the boundary of the confinement move in an opposite direction from the bulk flow of the cells nearer the center of the microenvironment. [7]

Chemotaxis. A change in the E. coli's environment may activate the tails' motion. Once a change is sensed with chemoreceptors on the cell's surface, the cell may choose to move away or towards an area. This phenomenon is termed chemotaxis. In this study, I sought to control the motility of E. coli by introducing chemicals to a bacteria-filled droplet. According to Julius Adler study in 1969, chemotaxis can be measured with a capillary assay (Figure 8). This assay requires bacteria suspended in an aqueous domain between a glass cover slip and a bent glass capillary tube. A chemoattractant-filled straight capillary tube is held in the bacteria suspension. Adler discovered a huge accumulation of E. coli at the tip and inside of glucose-filled capillary tubes [30]. However, his method did not test the control, which is whether the cells would prefer to

accumulate at the tip of a capillary tube not filled with a chemoattractant. I have designed two new methods for measuring the chemotaxis of bacteria in the presence of a chemoattractant. These new systems allowed me to monitor motility based off conflicting environmental conditions. More details will be provided in the subsequent chapters.

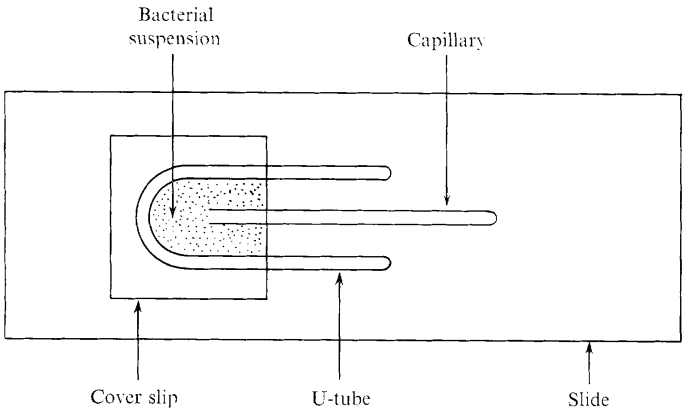

Figure 8 - Chemotaxis Assay Apparatus.

CHAPTER 3

HYPOTHESIS AND OBJECTIVES

3.1 Hypothesis

In this study, I challenged the DIB system's voltage dependency in order to expand its capabilities as a model cellular membrane. This study viewed the droplet as a microenvironment for microbial interactions, especially the interactions of *E. coli*. The study also used the adaptability of the DIB to form stable lipid bilayers. Typically bacteria interact with cellular membranes. This fact motivated the hypothesis: "Bacteria will prompt active responses of interfacial bilayer transduction pathways and membrane surfaces." The result of this research may greatly influence the understanding of the DIB technique.

3.2 Objectives

The guiding research study is bacteria and model membrane responsiveness upon interaction. This involves the following specific objectives:

1. To design a stable interface bilayer separating bacteria and a chemoattractant
2. To characterize the bacterium motility in a three dimensional microenvironment
3. To examine the interactions between the bacterium and the membrane.

CHAPTER 4

MEMBRANE-BACTERIA INTERACTION EXPERIMENTAL DESIGN

The cell membrane's phospholipid bilayer and extensive biomolecules influence the structure of our cell, the interaction with other cells, and the function of the organelles within our cells. The next section provides a new approach for studying the model cell membrane's responsiveness upon interaction with other cells, like *E. coli*, a common cell invader in the natural world. The DIB technique serves as the model cell membrane.

4.1 DIB Network and Platform Fabrication

Nanoliter aqueous droplets coated with lipid monolayers were arranged into a cell network and held in an oil reservoir with silver-silver chloride (Ag/AgCl) electrodes (Figure 9).

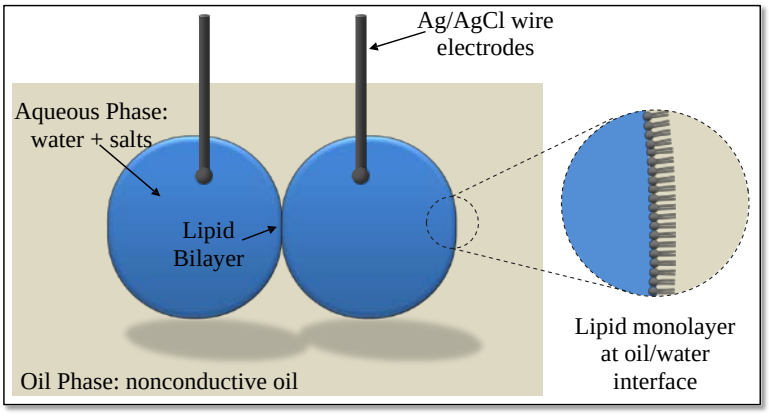

Figure 9 - DIB Setup. Aqueous droplets submerged in oil with Ag/AgCl wire electrodes

Then, strong Van der Waals interactions between the hydrophobic tails of the lipids caused neighboring droplets to connect and form a bilayer. The droplet contents were bacteria suspended in a buffer solution, and the droplets were coated with 1,2-

diphytanoyl-sn-glycero-3-phosphocholine (DPhPC) lipids (Avanti Polar Lipids, Inc.) or poly(dimethylsiloxane-co-ethylene oxide) triblock copolymers (Polymer Source, Inc.), which were used to demonstrate the applicable potential of the DIB technique. In order to induce activation at the interface bilayer, a DC voltage was applied to the droplets with a function generator. The DIB technique helped to independently control the content and size of the droplets, given the use of manual manipulators and manual microinjectors.

This work utilizes an oil-filled PDMS-glass substrate. A PDMS mold was created from a 3D printed master. A 1 to 10 ratio of PDMS to curing agent was well mixed and poured into a mold-release sprayed master. The mix was then set in a 60°C oven for 2.5 to 3 hours. After cooling to room temperature, the mold was peeled out of the master and placed, along with a glass slide, into a plasma cleaner (Harrick Plasma) for 20 seconds at the highest intensity (Figure 10). The plasma cleaner turned the mold from hydrophobic to hydrophilic and enhanced the bond strength between the PDMS and the glass slide. If the PDMS mold partially adhered or became unattached from the slide, then PDMS gel was injected in between the PDMS mold and the glass slide then heat cured for 2 hours. A durable platform was fabricated from this technique.

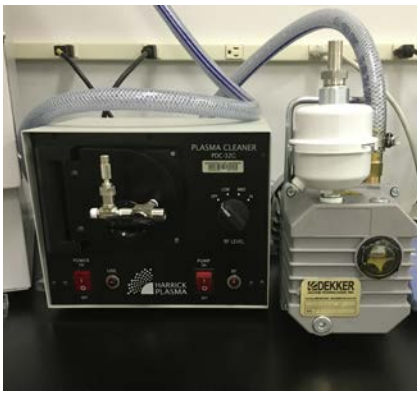

Figure 10 - Plasma Cleaner.

4.2 DIB Network and Platform Fabrication Materials

Base. A thin 2.4 cm x 4.0 cm x 0.1 cm glass slide was used as the base of the platform. The thin glass slide has a very smooth, leveled surface. However, constant usage caused the slide to bend. To maintain a level surface, the glass slide was replaced after each trial. Essentially, the thin glass was used to improve perception of the micron-sized *E. coli* over an inverted microscope.

PDMS. PDMS, better known as silicone rubber, is an extremely versatile polymer. A substrate of this material is favored for its excellent flexibility and stability. The polymer also has a low glass transition temperature, Tg, of -125°C [31]. Above this temperature the polymer is rubber whereas below the Tg, the polymer is glassy. A glassy behavior affects the polymer's ability to change its conformation. The temperature was maintained at room temperature, 22°C. Other materials, like polyurethane rubber or polyethylene glycol, were tested in this study. However, PDMS offered better durability and stability with the DIB setup. PDMS was also the optimal material for its ease of fabrication and flexibility (Table 1).

PDMS Mold. The PDMS mold consisted of a 1 to 10 weight-to-weight mixture of a Silicone Elastomer curing agent and a base (Dow Corning). The mixture was stirred gently and then poured into the master to evenly distribute the curing agent. This was then put in a vacuum chamber at -50kPa for 20 minutes to remove any air bubbles that accumulated from mixing. The mold had a 1 cm height, 3 cm width and length, and center radius of 0.75 cm, and 0.45 cm thickness. The mold was cured after heating to approximately 60°C in a VWR oven. Varying the temperature to a higher degree caused the mold to cure faster, and a lower degree caused the mold to have a rough and sticky

texture, which could be cleaned and smoothed with 80% Ethyl Alcohol (Sigma Aldrich). Workable PDMS molds were smooth and did not contain rips or air bubbles.

DIB Composites. DPhPC lipids were used to form stable membranes. Similar to all lipids, DPhPC has a hydrophilic head group and a hydrophobic chain[32]. The head group contains a charged group, making it polar. This characteristic enabled the head group to interact with water and shield the apolar tails from water. The lipids arranged around aqueous droplets in an ordered structure, also known as the crystalline lipid phase [33].

The triblock copolymers were also used as a water droplet coating in the trials. They were an ordered, rigid structure at about room temperature, approximately 22.75°C. However, since the molecules melt at a higher temperature 52.72°C, the polymers precipitated during experimentation. Just the same, the melted copolymers and the precipitated copolymers were used to form stable membranes.

The aqueous domains of the droplets were composed of a buffer solution of salt ions, amino acids, or pure sugars. The solutions were a mixture of either 10mM 4-Morpholinepropanesulfonic acid (MOPS), potassium chloride (KCl), and Glucose or 10mM KCl and 5% or 10% Casamino Acids.

The oil phase contained similar aliquots of Hexadecane and Silicone AR 20 oil. The mixture was close to the density of water, thus limiting the gravitational effects. The lipids readily dissolved in the oil phase to a concentration of 2 mg/mL, and quickly assembled on the oil-water interfaces when water droplets were introduced to the oil.

Electrodes. The silver-silver chloride (Ag/AgCl) electrodes held the droplets in place and allowed for electrical measurements. The electrodes were made with 0.125 mm

diameter silver wires. The wires were set in bleach, a chloride ion rich solution, for 30 minutes, or until they appeared as a uniformly distributed dull-gray color that contrasted the original bright silver color of the wire. This step provided a AgCl coating on the silver wires for improved conduction of a voltage across the membrane. After being rinsed with water, one end of the electrodes was dipped in 2.0% agarose in order to form a small bead of gel on the electrode tip. The agarose is a hydrophilic gel that provided a point of adhesion for the droplets (Table 1). The beaded wire electrodes delivered an electron current from the membrane to the measurement devices, Multiclamp 700B and Digidata 1550 (Axon CNS Molecular Devices).

Table 1 - Classes of Biomaterials

Biomaterial	Classification	Description
PDMS	Synthetic Homopolymer	Less temperature sensitive, high flexibility and stability
Polyurethane	Synthetic Copolymer	Rubbery, tough elastomers with good fatigue and blood containing properties
Polyethylene glycol	Synthetic Hydrogel	Insoluble in water, versatile physical properties
Agarose	Natural Hydrogel	Insoluble in water, provides mechanical support for cells

Devices. Multiclamp 700B, Digidata 1550, and a function generator (Hewlett Packard) were devices used to control and monitor the conductance properties, such as voltage and current (Figure 11). They were excellent tools for studying membrane electrophysiology

and channel activation behaviors. For this experiment, the function generator was used to apply a 10 millivolt (mV) peak-to-peak triangle-wave voltage to the DPhPC lipid bilayers and apply a 10 mV peak-to-peak triangle wave held at 200mV to the triblock copolymer lipid bilayers. The function generator was connected to the Multiclamp 700B device with a BNC cable. A head stage was then connected from the back of the apparatus to the electrodes. BNC cables were then used to connect the Multiclamp 700B to the Digidata 1550. The computer software Axoscope displayed the current and voltage recordings in a graphical representation. The computer software Multiclamp 700B commander communicated with the patch-clamp device via a USB interface. The software could report and control voltage, current, and resistance measurements. With the commander, the proper scaling factors for the device were ensured. (Appendix A: Electric Field in the DIB)

Figure 11 - Multiclamp 700B (top) and Digidata 1550 (bottom).

4.3 Bacteria Cultivation

Cultivation. Strains XL-1 Blue and RP437 were inoculated for 8-12 hours in a test tube filled with 3 mL of Luria Bertani broth on a 37ºC 290 rpm shaker incubator (Figure 12).

The cells were next plated and streaked on a LB-agar plate, then placed in an incubator oven in order to form isolated colonies (Figure 13). Signs of contamination, like different colored or textured colonies, could be detected at this stage.

Transformation. To prepare the competent cells, *E. coli*, XL1-Blue or RP437, was inoculated in 3 mL LB broth and grown over night at 37 ℃. 2% (60 µL) XL1-Blue overnight culture was then added into 3 mL LB media. When the OD_{600} of bacterial cell culture is 0.4, the culture was poured into a centrifuge tube and kept on ice for 10 minutes. Then, the culture was centrifuged at 4 ℃ for 3 minutes at 4000 rpm (Figure 14). Cells were washed two times with 3 mL CCB1 buffer, then the pellet was re-suspended in 100 µL ice cold CCB1. After being chilled over ice for 20 minutes, the cell membranes of the competent cells were more permeable and prepared for transformation, which is a genetic modification of the bacterium by incorporating DNA of a different bacterial cell.

The XL1-Blue and RP437 competent cells were transformed by the heat shock method. 2 µL of pZE-enhanced Green Fluorescent Protein (pZE-eGFP) plasmids were added into the culture and kept on ice for 20 minutes. Then, the bacterial cells were heated in a 42 ℃ water bath for 90 seconds and then incubated on ice for 2 minutes. 700 mL of fresh LB broth was added to the culture. Then the cultures were kept in a 37 ℃ shaker for 40 minutes to recover the cells. After centrifuging the cells at 4000 rpm for 4 minutes, the remaining pellets at the bottom of the tube were re-suspended with 100 µL of LB broth and plated on the LB agar plate with ampicillin, then placed in a 37 ℃ incubator oven. If there were no signs of contamination, an overnight single colony from the LB agar plate was inoculated in 3 mL LB broth with 3 µL 100 mg/L ampicillin and 3

μL 0.5 mM Isopropyl β-D-1-thiogalactopyranoside (IPTG) (Zymo Research) at 290 rpm for the eGFP fluorescence assay.

Figure 12 - 37ºC, 290rpm Shaker Incubator.

Figure 13 - 37ºC Incubator Oven.

Figure 14 - Centrifuge used to spin cells at low 4ºC temperatures.

Fluorescence Assay. To measure eGFP fluorescence in liquid media, transformed cells were cultured in 3.5 mL LB medium with 100 mg/L of ampicillin and 1 mM IPTG at 37 °C and set in shake incubator at 290 rpm overnight. Then a 3 µL culture was diluted 1000 fold and 1 µL of the diluted solution was dropped into a PDMS-glass substrate to detect the fluorescence signal using an inverted fluorescence microscope (Leica) with the GFP filter cube (470/40 nm excitation, 495 nm emission) (Figure 15).

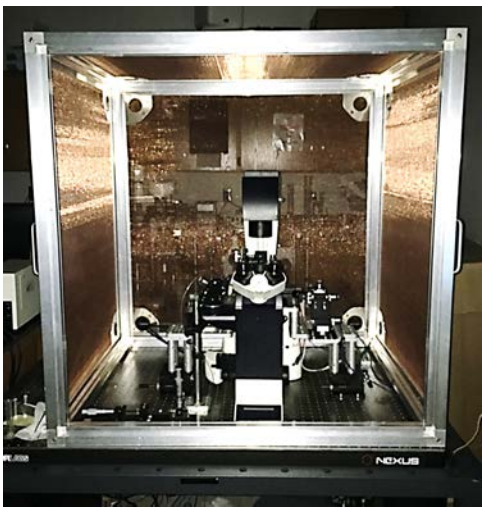

Figure 15 - Leica Microscope for Fluorescence Microscopy.

***E. coli* Motility Test.** The motility of the *E. coli* was tested using the hanging drop test. A 500 µL aliquot of the *E. coli* overnight culture was centrifuged at 8000 rpm for 1 minute (Figure 16). The supernatant was removed and the remaining pellets were washed with a medium containing 100 mM Potassium Phosphate, pH 7.0, and 1 mM Ethylenediaminetetraacetic acid (EDTA). EDTA was needed to restore the motility to the cells [34]. After three wash cycles, the pellets were gently re-suspended in 10mM Glucose with a micropipette. A droplet of the suspended cells was then placed in the center of a vacuum greased plastic ring on top of a glass slide. A second slide was placed on top of this. The entire apparatus was then flipped, creating a hanging drop. The drop containing the motile cells was seen using a Leica microscope's 63X objective. Motility was confirmed by the speedy random walk and swimming motion of the cells.

Figure 16 - Centrifuge used to separate *E. coli* cells from the aqueous supernatant.

Chemotaxis Assays. Soft agar-LB assays and the two-point capillary assay were developed to study *E. coli* chemotaxis. Both methods tested the *E. coli's* affinity for a chemoattractant.. In the soft agar-LB assays, 2 holes were made about 2 cm apart on 0.2% soft agar-LB plates. 100 µL of an overnight culture of RP437 was placed in one hole, while a chemoattractant, 10mM Glucose, 20mM Glucose, 100mM Glucose, or 10% Casamino Acids, was placed in the other hole. The plates were placed in a 37°C incubator oven for 20 hours. The chemoattractant was a chemotaxis stimulus if the *E. coli* cells grew at a greater concentration towards the attractant and grew at a lower concentration in other directions. If the *E. coli* cells did not have a chemotactic response, they grew in all directions at the same concentration. In result, the *E. coli* RP437 grew at a higher concentration in the directions of 20 mM and 100 mM Glucose than any other direction on the plate. There was no difference in the *E. coli* strain's directional growth patterns in the presence of 10 mM Glucose and 10% Casamino Acid.

The Two-Point Capillary Assay Technique was designed by inserting two filled capillary tubes in the well of a PDMS-glass substrate. The capillary tubes were filled, one with a chemoattractant, 27.8 mM glucose, and the other with deionized water. The well was filled with starved *E. coli* cells. The starved cells were prepared with cells from an 8-hour inoculation period of RP437. A 200 µL cell sample was removed from the inoculation tube and centrifuged at 8000 rpm for 1 minute. The cells were washed three times and then re-suspended with 200 µL of the wash medium. Then, the suspension was injected into the well. A second glass slide covered the well and prevented immediate evaporation of the suspension. The well was set on a 30°C heating stage for 3 hours. Diffusion of the chemoattractant around the tip of the capillary tube caused the cells to

accumulate at the tip and then swim inside the tube. The contents of the tube were inoculated in LB broth for 4 hours then estimated with an OD_{600} spectrophotometer, which was able to estimate the concentration of *E. coli* cells in the LB broth measured at a wavelength of 600 nm. The OD_{600} of both the glucose and the water was 0.027 and 0.023 respectively. This meant the glucose-filled tube attracted approximately 2.16×10^7 bacterial cells/mL while the water-filled tube attracted nearly 1.84×10^7 bacterial cells/mL. There was not a substantial difference between the *E. coli's* attraction to the chemoattractant and the water. This method may be improved by replacing the water with a repellent in order to better characterize the *E. coli's* behavior.

4.4 Bacteria Cultivation Materials

Strains. The *E. coli* strain XL1-Blue is a mutant of the parent strain BW25113. This strain has resistance to the antibiotic tetracycline [35]. The *E. coli* strain RP437 is a chemotactic wild-type *E. coli* K-12 Strain [36, 37]. The strain has resistance to the antibiotic streptomycin [38]. The antibiotics could be added to the cultures to prevent the growth of other strains during the experiment. Plasmid DNA extracted from other transformed cells using a miniprep protocol (Appendix B: DNA Plasmid Preparation) was added to competent cells of each strain for transformation (Table 2).

Table 2 – Bacteria Description

Strain	Genotype	Source
XL1-Blue	*recA1 endA1 gyrA96 thi-1 hsdR17 supE44 relA1 lac [F ′ proAB lacIqZΔM15 Tn10 (Tetr)]*	Stratagene
RP437	*thr-1*, *araC14*, *leuB6*(Am), *fhuA31*, *lacY1*, *tsx-78*, *λ⁻*, *eda-50*, *hisG4*(Oc), *rfbC1*, *rpsL136*(strR), *xylA5*, *mtl-1*, *metF159*(Am), *thiE1*	Coli Genetic Stock Center
Plasmid	**Description**	**Reference**
pZE12-luc	$P_L$lacO1, *colE* ori, *luc*, Amp^r	[5]
pZE-eGFP	pZE12-luc harboring gene *egfp* from pEGFP-N1 Vector	This Study

Growth Medium, Growth Conditions, and Buffers. The broth that ensures optimal *E. coli* growth and DNA plasmid preparation is Luria Bertani (LB) [30]. An LB stock solution is made of 10 g trypton, 10 g potassium chloride, and 5 g yeast extract dissolved in 1 L deionized water. This stock solution was autoclaved for 20 minutes then transferred into glass test tubes at 3 mL each. The cells grow best in an incubator oven or shaker set at a temperature of 37°C, an optimal condition for the *E. coli* [39, 40]. In this condition, the cells reached an OD_{600} of about 0.4, or concentration of 3.2×10^8, after 12 hours of incubation. The cells were active when grown to this concentration. After incubation, competent cells were washed and stored with buffers, CCB1 and CCB2 respectively. CCB1 contained 5.15 g Calcium Chloride (CaCl) per 200 mL of milli-Q water (Millipore Corporation). The mixture was autoclaved for 40 minutes. A steam autoclave, heating to over 100ºC, sterilized both the growth medium and buffers. Therefore, foreign particulates could not affect the growth of the *E. coli* strains. Once cooled down, 2.5mL of 1 M Magnesium Sulfate ($MgSO_{4)}$ was added. The $MgSO_4$ caused the membrane of the *E. coli* cells to become vulnerable and prepared to receive a plasmid in the transformation steps following. CCB2 is similar to CCB1 except that it was prepared with only 1mL $MgSO_4$ and 72 mL glycerol. The *E. coli* cells were stored at a 1:1 concentration with the CCB2 buffer in a -80ºC freezer. After the competent cells were transformed with the DNA plasmids, adding a small aliquot of IPTG, an inducer molecule, enhanced the expression of the green fluorescent protein.

Motility Medium and Soft Agar. The type of motility medium and agar concentration influenced how well the *E. coli* cells respond to a chemoattractant. The motility medium was kept at a low ion concentration and without a food source to ensure maintenance of

cell motility throughout the chemotaxis and motility tests. The agar was made at a low concentration of 0.2% wt/vol of LB broth. The cells move faster and travel further in soft agar environments [34, 41].

4.5 Bacteria Encapsulation in Droplets

The XL1-Blue and RP437 bacterial cells were inoculated separately for 8 hours. The RP437 culture was then centrifuged at 8000 rpm for 1 minute so the supernatant could be removed and the remaining pellets re-suspended in 10 mM Glucose. The XL1-Bue and the re-suspended RP437 cells were then diluted 1000-fold in a buffer solution of 10 mM Glucose, KCl, and MOPS, pH7.4. According to Adler's studies on chemotaxis, cells tend to lose their motility when ion concentrations are above 10 mM [34]. An energy source, like glucose sugars, kept the cells visually active and motile until oxygen levels depleted. A sharpened capillary tube was filled with the *E. coli*-buffer solution. Next, motile bacteria within emulsion as well as emulsions containing a chemoattractant were depositing into a PDMS-glass substrate (Table 3). The substrate contained an oil reservoir with dissolved DPhPC lipids or triblock copolymers. Prior techniques involved dissolving the lipids and copolymers in the aqueous phase (Appendix C: Lipids Preparation Protocols). The droplets were then brought into contact to form a bilayer (Figure 17). The net result was a complex stimuli-responsive network that allowed for seeking through the motion of the captured *E. coli* bacteria. The movement of the bacteria was observed through fluorescence microscopy. The motility within the droplets was studied with Leica software, tracked with a particle tracker on ImageJ or Open Source Physics software, and illustrated with MATLAB algorithms and Microsoft Excel.

Table 3 – Asymmetric Droplet Contents

Reagent/Species	Droplet A	Droplet B	Source
KCl	10 mM	10 mM	Sigma Aldrich
MOPS	20 mM	10 mM	Sigma Aldrich
Casamino Acids	0.4% w/vol	None	Amresco
Glucose	None	10 mM	Sigma Aldrich
XL1-Blue	1000 fold dilution	None	This study

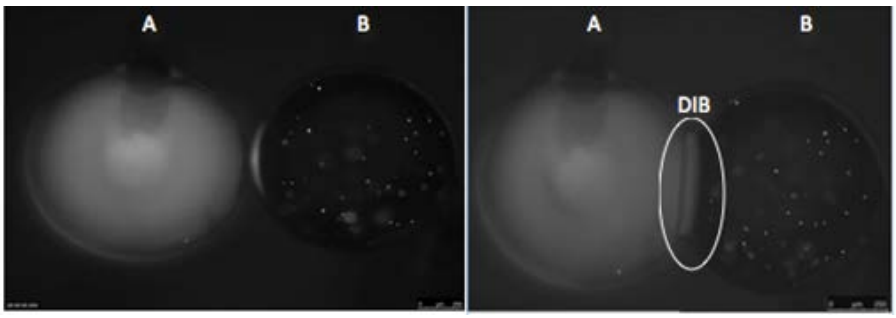

Figure 17 – Droplet-Droplet Contact. The droplets contained a buffer solution with bacterium (Droplet B) or a chemoattractant 0.4 % Casamino Acids (Droplet A). The Bacteria was diluted 1000 fold with the Glucose-containing buffer solution and then made into a droplet. The Casamino Acids-containing droplet was placed in a neighboring droplet. The droplets were brought into contact to form a DIB.

CHAPTER 5

RESULTS AND DISCUSSION

The Droplet Interface Bilayer technique suits studies of the lipid bilayer. Results of the described methodology revealed the artificial membrane's physiological relevance, predictive capabilities, and ease-of modification. The membrane served as a stable barrier between aqueous droplets. The contents of the droplets were not able to diffuse across the membrane easily since the membrane is innately selectively permeable. Also, the chemoattractant and *E. coli* sizes are too large to naturally diffuse across without a membrane protein channel. Stimuli-responsive *E. coli* mobilized in this confined three-dimensional environment. In a DPhPC coated droplet, sudden changes, like membrane formation and collapse, may have affected *E. coli* trajectory and speed. The *E. coli* swam swiftly towards the membrane as it formed and widened (Figure 18). The cells exhibited a directional trend in the droplets. The *E. coli* became inert as the membrane stabilized to an optimal size. This effect on the *E. coli* may have been due to a decrease in the oxygen levels inside the droplets. Triblock copolymer coated droplets had comparable stability to DPhPC coated droplets. In the triblock copolymer coated droplets, motile *E. coli* RP437, were observably active (Figure 19 - Figure 21) until either oxygen levels depleted or after membrane formation in the droplets. Oxygen levels tend to decrease in such confinements, which affects the viability of the *E. coli* [28]. The total distance the bacteria traveled was used to study the trajectory of the cells. In addition, the average speed was used to measure how fast the cells traveled a particular distance in a short span

of time. Then, an analysis of the average velocity provided information about the rate at which the cells changed position as well as the directional tendency of the cells. XL1-Blue cells were non-motile and therefore diffused across an aqueous reservoir at an average distance of 103 μm, an average speed of 1.6 μm/s, and an average velocity of 0.047 μm/s, 53º East of North. Motile, RP437 bacterium swam at a distance of 187 μm, an average speed of 3.0 μm/s, and an average velocity of 0.83 μm/s, 78º East of North. According to Howard Berg, bacteria with flagellum swim on average at a speed of 30 diameters per second if the flagella is revolving at 100 revolutions per second [27]. Without knowledge of the flagellum's actions, the *E. coli* were assumed to move between 10 and 30 diameters per second. Typically, bacteria are 1-2 micrometers (μm) in diameter [42]. Therefore, in 60 seconds, the cells were anticipated to move between 600 to 1800 μm. The cells in this study changed velocity rapidly due to the confined space and surface boundary of the droplets. In an 839 μm diameter DPhPC coated droplet without a chemical gradient, the XL1-Blue cells drifted at an average distance of 820 μm, an average speed of 13 μm/s, and an average velocity of 0.81 μm/s, 70º East of North. On the other hand, the RP437 cells swam in an 1812 μm diameter triblock copolymer coated droplet at a distance of 1126 μm, an average speed of 17 μm/s, and an average velocity of 2.3 μm/s, 35º West of South. In a droplet with a chemical gradient introduced at a lipid or copolymer bilayer, the average speed and velocity was 9.6 μm/s and 1.2 μm/s, 85º West of North for non-motile cells moving towards the lipid bilayer of a 1135 μm diameter droplet and 2.8 μm/s and 0.71 μm/s, 15º East of North for motile cells moving away from the copolymer bilayer of a 643 μm diameter droplet. Non-motile cells drifted in the direction of the convective flow instead of in response to the bilayer.

Motile cells swam in random directions regardless of the bilayer. After the collapse of the DPhPC lipid bilayer, the cells tended to speed up and vortex around the droplet, this behavior was noted in previous experiments of Wioland and Lushi [7, 29]. However, the motile cells in the triblock copolymer coated droplets became inactive after the bilayer collapsed. In each circumstance, the cells were tracked for about 60 seconds. The displacements and speeds of the XL1-Blue and the RP437 in the aqueous environments closely match the expected trajectories and rates. Yet, the speed varied in confined environments due to varying factors, such as lack of oxygen or energy and the size of the droplet area. Moreover, bilayer instability truncated the chemoattractant perfusion. The results proved that the DIB technique provides a suitable model for studies of cell interactive behavior with the cell membrane and within confined environments.

The discovery of membrane behaviors and cell-to-cell interactions via a model lipid bilayer offers a high merit to the biological engineering field of study. Characterizing stimuli responsiveness of motile bacteria at a lipid bilayer, leads to further discoveries accomplished through a DIB network, wherein an encapsulation of motile bacteria may allow for stimuli responsiveness.

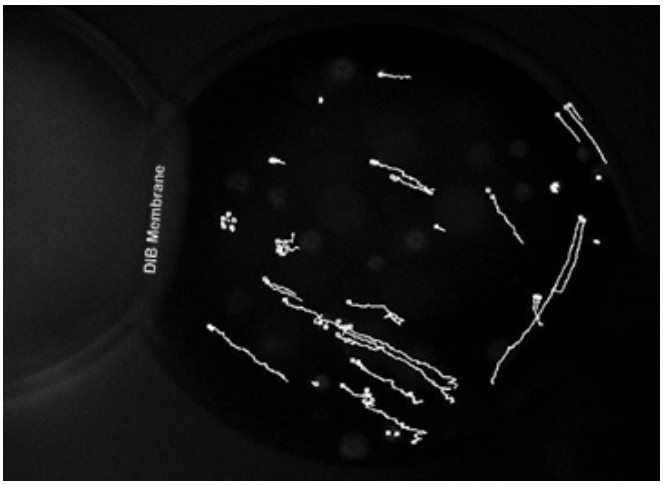


```
%% Bac1
mu_x = mean(A(1:21,1));  %average of distance traveled in
20 frames
mu_y = mean(A(1:21,2));
mcx_bac1 = (A(1:21,1) - mu_x)/.54;  %converting from pixels
to micrometers
mcy_bac1 = (A(1:21,2) - mu_y)/.54;
plot(mcx_bac1,mcy_bac1,'b')
hold on
d1 = sqrt((A(1,1) - A(21,1))^2 + (A(1,2) - A(21,2))^2);
v1 = d1/20;  %speed of bacteria given 1 frame/second
```

Figure 18 – Tracking *E. coli* in a Droplet. ImageJ counted each bacterium as a pixel and tracked the movement of each pixel in a sequence of fluorescent microscopy images from Leica software. The pixel data was then saved in Excel and loaded into MATLAB for analysis. A MATLAB algorithm was used for calculating displacement, distance traveled and velocity of the bacterium. Here we see several *E. coli* bacterium swimming in unison towards the membrane.

Inside Droplet – RP437 Bacterium 1

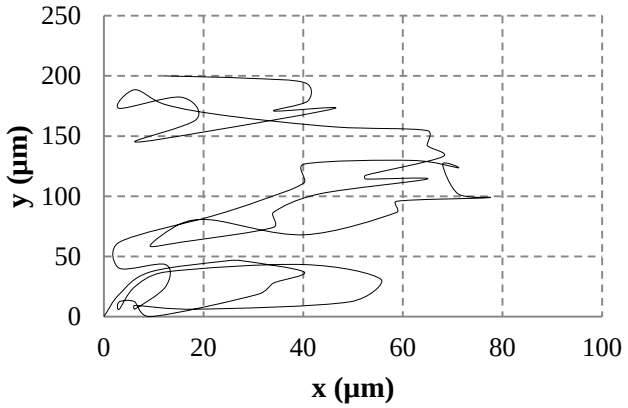

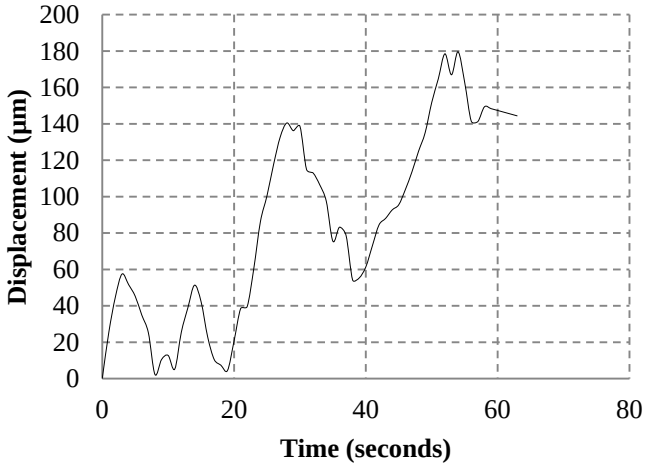

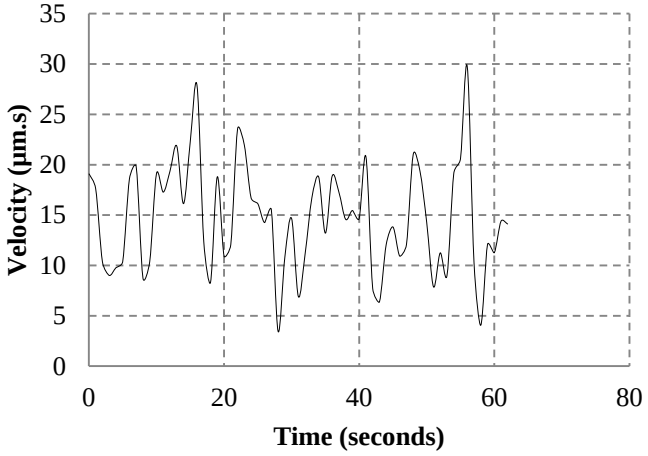

Figure 19 - Bacterium 1 in a Droplet without a Chemical Gradient Present

Inside Droplet – RP437 Bacterium 2

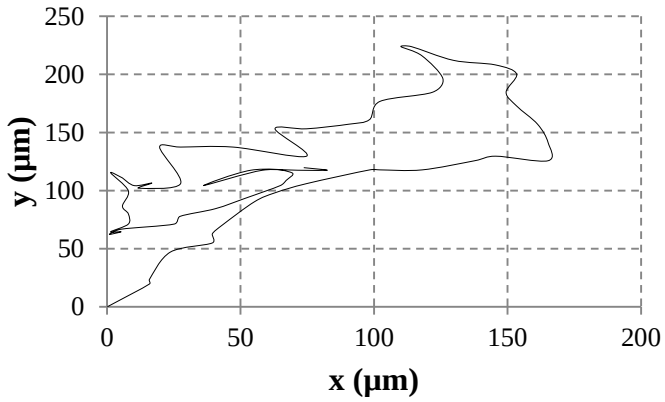

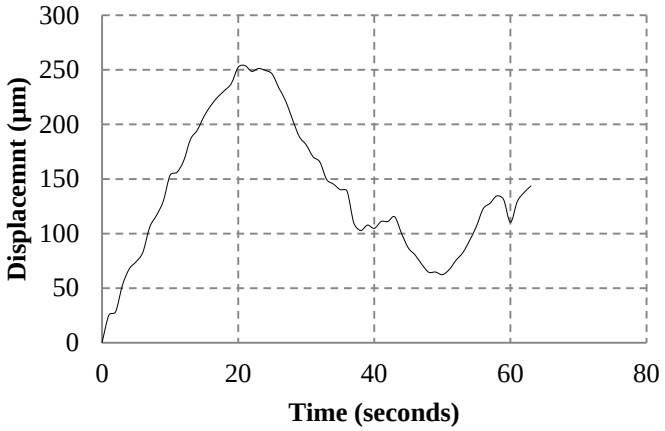

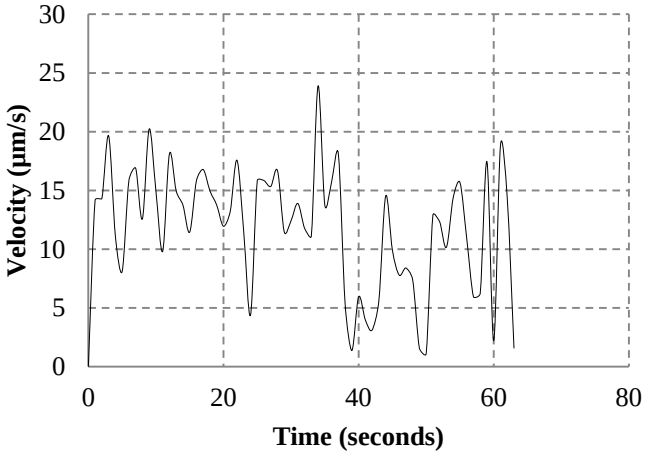

Figure 20 - Bacterium 2 in a Droplet without a Chemical Gradient Present

Inside Droplet – RP437 Bacterium 3

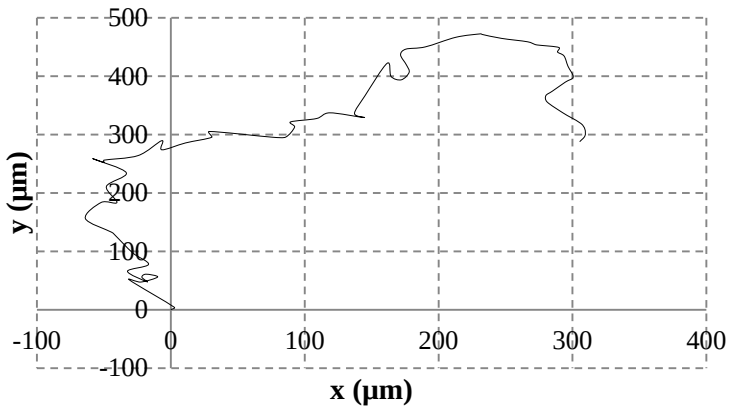

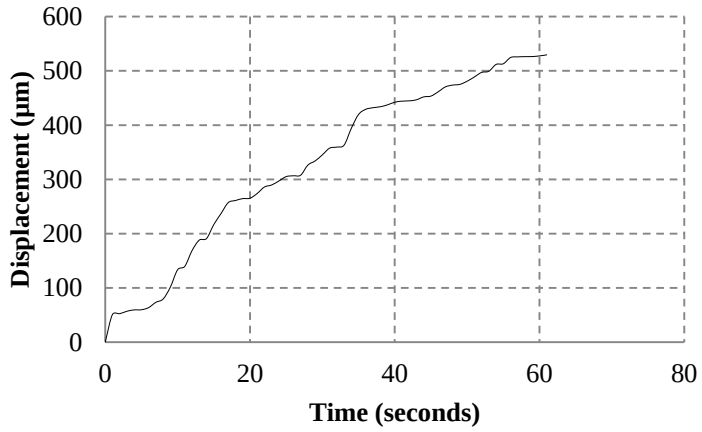

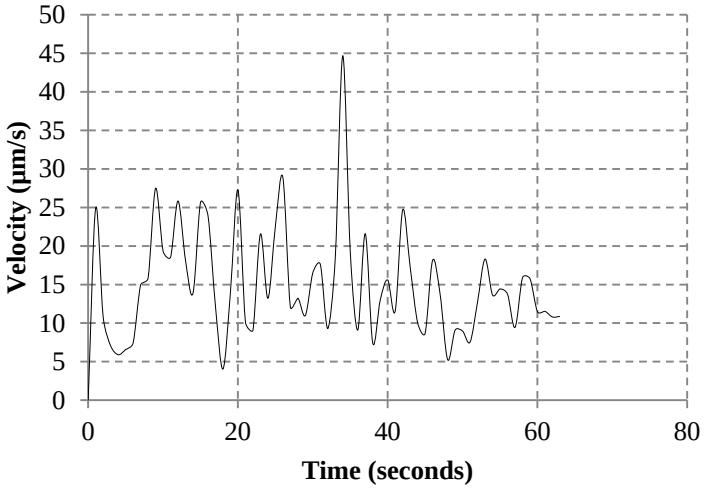

Figure 21 - Bacterium 3 in a Droplet without a Chemical Gradient Present

CHAPTER 6

SUMMARY AND CONCLUSION

Motile, stimuli-responsive bacteria may be useful tools for creating organic smart materials. This work encapsulates stimuli-responsive bacteria into a synthetic cellular system called a DIB network. The top-down approach joins with the bottom-up approach for synthetic biology in order to induce additional material responses in the DIB network. Motile *E. coli* bacteria serve as a model organism in this work. DPhPC Lipid and Triblock Copolymer coated droplets successfully encapsulate *E. coli* strains XL1-Blue and RP437. Fluorescent microscopy captures the motility of the cells transformed with eGFP. This visual marker allows for characterization of their trajectories within confined microfluidic environments. In observation, the motile bacteria swam in collective trajectories within the droplets due to generated hydrodynamic effects. In the work, the droplets became building blocks of an interfacial bilayer that separates *E. coli* from a chemoattractant, or chemical. *E. coli* seek chemicals, like glucose and casamino acids, on 0.2% soft agar-LB chemotaxis assays. The *E. coli* move readily in response to chemical changes in the environment. Given the interface bilayer's physiological relevance to the natural cell membrane, neither the *E. coli* nor the chemoattractant could permeate through the bilayer easily. The bacterial cells' motion may increase after the introduction of a chemoattractant, but more studies are required. A long-lasting stable interfacial membrane is crucial for this work, and experimental modifications are necessary.

REFERENCES

1. *The Cell Membrane*. Available from: www.sp.uconn.edu\~terry/images/cell/bilayer.gif.
2. Heimburg, T., *Thermal biophysics of membranes*. 2008: John Wiley & Sons.
3. Sarles, S.A., *Physical encapsulation of interface bilayers*. 2010, Virginia Polytechnic Institute and State University.
4. Taylor, G.J. and S.A. Sarles, *Heating-enabled formation of droplet interface bilayers using Escherichia coli total lipid extract.* Langmuir, 2014. **31**(1): p. 325-337.
5. Lin, Y., et al., *Microbial biosynthesis of the anticoagulant precursor 4-hydroxycoumarin.* Nature communications, 2013. **4**.
6. Weitz, M., et al., *Communication and computation by bacteria compartmentalized within microemulsion droplets.* Journal of the American Chemical Society, 2013. **136**(1): p. 72-75.
7. Wioland, H., et al., *Confinement stabilizes a bacterial suspension into a spiral vortex.* Physical review letters, 2013. **110**(26): p. 268102.
8. Chakrabarti, A.C. and D.W. Deamer, *Permeability of lipid bilayers to amino acids and phosphate.* Biochimica et Biophysica Acta (BBA)-Biomembranes, 1992. **1111**(2): p. 171-177.
9. Bangham, A.D. and R. Horne, *Negative staining of phospholipids and their structural modification by surface-active agents as observed in the electron microscope.* Journal of molecular biology, 1964. **8**(5): p. 660IN2-668IN10.

10. Mezei, M. and V. Gulasekharam, *Liposomes-a selective drug delivery system for the topical route of administration I. Lotion dosage form.* Life Sciences, 1980. **26**(18): p. 1473-1477.

11. Kiessling, V., J.M. Crane, and L.K. Tamm, *Transbilayer effects of raft-like lipid domains in asymmetric planar bilayers measured by single molecule tracking.* Biophysical journal, 2006. **91**(9): p. 3313-3326.

12. Marcus, A.J., H.L. Ullman, and L.B. Safier, *Lipid composition of subcellular particles of human blood platelets.* Journal of lipid research, 1969. **10**(1): p. 108-114.

13. O'Brien, J.S. and E.L. Sampson, *Lipid composition of the normal human brain: gray matter, white matter, and myelin.* Journal of lipid research, 1965. **6**(4): p. 537-544.

14. Montal, M. and P. Mueller, *Formation of bimolecular membranes from lipid monolayers and a study of their electrical properties.* Proceedings of the National Academy of Sciences, 1972. **69**(12): p. 3561-3566.

15. Bayley, H., et al., *Droplet interface bilayers.* Mol Biosyst, 2008. **4**(12): p. 1191-208.

16. Keller, B.U., et al., *Sodium channels in planar lipid bilayers. Channel gating kinetics of purified sodium channels modified by batrachotoxin.* The Journal of general physiology, 1986. **88**(1): p. 1-23.

17. Leonenko, Z., A. Carnini, and D. Cramb, *Supported planar bilayer formation by vesicle fusion: the interaction of phospholipid vesicles with surfaces and the effect*

of gramicidin on bilayer properties using atomic force microscopy. Biochimica et Biophysica Acta (BBA)-Biomembranes, 2000. **1509**(1): p. 131-147.

18. Kiessling, V.Y., Sung-Tae; Tamm, Lucas K, *Lipid Domains*. 19 ed. Current Topics in Membranes, ed. R.S. Balaban, Sidney A. Vol. Volume 75. 2015: Elsevier Inc. 1 - 19.
19. Goennenwein, S., et al., *Functional incorporation of integrins into solid supported membranes on ultrathin films of cellulose: impact on adhesion.* Biophysical journal, 2003. **85**(1): p. 646-655.
20. Visco, I., S. Chiantia, and P. Schwille, *Asymmetric supported lipid bilayer formation via methyl-β-cyclodextrin mediated lipid exchange: influence of asymmetry on lipid dynamics and phase behavior*. Langmuir, 2014. **30**(25): p. 7475-7484.
21. Tamaddoni, N., E.C. Freeman, and S.A. Sarles, *Sensitivity and directionality of lipid bilayer mechanotransduction studied using a revised, highly durable membrane-based hair cell sensor.* Smart Materials and Structures, 2015. **24**(6): p. 065014.
22. Sundaresan, V.B., et al., *Biological transport processes for microhydraulic actuation.* Sensors and Actuators B: Chemical, 2007. **123**(2): p. 685-695.
23. Xu, J., F.J. Sigworth, and D.A. LaVan, *Synthetic protocells to mimic and test cell function.* Advanced Materials, 2010. **22**(1): p. 120-127.
24. Dunne, C., *Adaptation of bacteria to the intestinal niche: probiotics and gut disorder.* Inflammatory bowel diseases, 2001. **7**(2): p. 136-145.

25. Martens-Habbena, W., et al., *Ammonia oxidation kinetics determine niche separation of nitrifying Archaea and Bacteria.* Nature, 2009. **461**(7266): p. 976-979.

26. Eckburg, P.B., et al., *Diversity of the human intestinal microbial flora.* science, 2005. **308**(5728): p. 1635-1638.

27. Berg, H.C., *Marvels of bacterial behavior.* Proceedings of the American Philosophical Society, 2006. **150**(3): p. 428-442.

28. Douarche, C., et al., *E. Coli and oxygen: a motility transition.* Physical review letters, 2009. **102**(19): p. 198101.

29. Lushi, E., H. Wioland, and R.E. Goldstein, *Fluid flows created by swimming bacteria drive self-organization in confined suspensions.* Proceedings of the National Academy of Sciences, 2014. **111**(27): p. 9733-9738.

30. Adler, J., G.L. Hazelbauer, and M. Dahl, *Chemotaxis toward sugars in Escherichia coli.* Journal of Bacteriology, 1973. **115**(3): p. 824-847.

31. Clarson, S., K. Dodgson, and J. Semlyen, *Studies of cyclic and linear poly (dimethylsiloxanes): 19. Glass transition temperatures and crystallization behaviour.* Polymer, 1985. **26**(6): p. 930-934.

32. *Avanti Polar Lipids, Inc.* [website]; Available from: https://avantilipids.com/product/850356/.

33. Luzzati, V. and F. Husson, *The structure of the liquid-crystalline phases of lipid-water systems.* The Journal of cell biology, 1962. **12**(2): p. 207-219.

34. Adler, J., *A method for measuring chemotaxis and use of the method to determine optimum conditions for chemotaxis by Escherichia coli.* Microbiology, 1973. **74**(1): p. 77-91.

35. Miller, L.P., J.T. Crawford, and T.M. Shinnick, *The rpoB gene of Mycobacterium tuberculosis.* Antimicrobial agents and chemotherapy, 1994. **38**(4): p. 805-811.

36. Liu, X. and R.E. Parales, *Chemotaxis of Escherichia coli to pyrimidines: a new role for the signal transducer Tap.* Journal of bacteriology, 2008. **190**(3): p. 972-979.

37. Parkinson, J.S., *Complementation analysis and deletion mapping of Escherichia coli mutants defective in chemotaxis.* Journal of Bacteriology, 1978. **135**(1): p. 45-53.

38. Jasuja, R., et al., *Chemotactic responses of Escherichia coli to small jumps of photoreleased L-aspartate.* Biophysical journal, 1999. **76**(3): p. 1706-1719.

39. Mattiuzzo, M., et al., *Role of the Escherichia coli SbmA in the antimicrobial activity of proline-rich peptides.* Molecular microbiology, 2007. **66**(1): p. 151-163.

40. Schulmeister, S., K. Grosse, and V. Sourjik, *Effects of receptor modification and temperature on dynamics of sensory complexes in Escherichia coli chemotaxis.* BMC microbiology, 2011. **11**(1): p. 222.

41. Croze, O.A., et al., *Migration of chemotactic bacteria in soft agar: role of gel concentration.* Biophysical journal, 2011. **101**(3): p. 525-534.

42. Männik, J., et al., *Bacterial growth and motility in sub-micron constrictions.* Proceedings of the National Academy of Sciences, 2009. **106**(35): p. 14861-14866.

APPENDIX A

ELECTRIC FIELD IN THE DIB

A.1 Denoising Techniques

To get a proper recording of the DIB activity, we had to get rid of any noise coming from the device-in-use or the surroundings. A copper mesh Faraday cage was used to keep any noise from the area (Figure 22). The cage and the microscope were also grounded to reduce their effects on the recordings. A grounding block was set inside the cage in order the ground the microscope, headstage, and cage. A filtering power supply was then utilized to the reduce the hum. A minimal noise level was achieved with this process.

Figure 22 - Denoising with a Farraday Cage.

APPENDIX B

DNA PLASMID PREPARATION

B.1 Miniprep Protocol

1. Inoculate a culture containing the desired DNA plasmid in a test tube of 3 mL LB
2. Centrifuge 2mL of the overnight culture from the previous step at max speed for three minutes
3. Resuspend cells with 600µL of deionized water
4. Mix in 100µL of blue lysis buffer and wait 30 seconds for the reaction to occur
5. Mix in 350µL of yellow neutralization buffer
6. Centrifuge mixture at max speed for three minutes
7. Transfer the supernatant to a spin column
8. Centrifuge at max speed for thirty seconds max
9. Add 200µL of Endowash buffer
10. Centrifuge at max speed for thirty seconds max
11. Add 400µL of Zippy wash buffer
12. Centrifuge at max speed for one minute max
13. Transfer spin column to microcentrifuge tube
14. Add 50µL of deionized water and wait for five minutes for reaction to occur
15. Centrifuge at max speed for thirty seconds max
16. Store in -20ºC freezer

APPENDIX C

LIPIDS PREPARATION PROTOCOLS

C.1 Steps for Lipids Dissolved in Water

1. Fill a vial of lipids with deionized water to a concentration of 2mg/mL
2. Do five freeze and thaw cycles
3. Fill a 1 mL Hamiltonian glass syringe with the lipid solution after pre-wetting the syringe with a buffer
4. Filter the lipids with an Avanti Polar Lipid Extruder until the solution is clear or after at least six passes through a pre-wet filter support
5. Sonicate the lipids for five minutes with an Avanti Sonication tub
6. Place a sample in a 4ºC refrigerator for short-term storage
7. Place the remaining solution in a -20ºC freezer for long-term storage

C.2 Steps for Triblock Copolymers in Oil

1. Weigh out 16 mg of triblock copolymer pellets
2. Add the pellets to a 50/50 solution of Hexadecane oil and Silicone AR 20 oil to a concentration of 4mg/mL
3. Heat slowly to 90ºC or until the pellets are completely dissolved
4. Cool the solution back down to 50ºC
5. Store in a dark place and cover with aluminum foil or electrical tape to shield the solution from the light